International Journal of Science and Research (IJSR)
ISSN: 2319-7064
SJIF (2022): 7.942

Heat Transfer Enhancement through Perforated Fin Made by Al-SiC-MMC and Optimization of Design Parameters using Taguchi DOE Method

A. Kalyan Charan[1], Dr. R. Uday Kumar[2], Dr. B. Balunaik[3]

[1]Assistant Professor, Dept. of Mechanical Engineering, Matrusri Engineering College, Saidabad, Hyderabad, India

[2]Associate Professor, Dept. of Mechanical Engineering, Mahatma Gandhi Institute of Technology, Gandipet, Hyderabad, India

[3]Professor Mechanical Engg & Director of University Foreign Relations, JNTUH, Hyderabad, India

Abstract: ***Aluminium silicon carbide metal matrix composites are employed in a wide range of applications, including aerospace, aviation, automobiles, turbine blades, and brake pads. Aluminum silicon carbide metal matrix composites can be made using a variety of manufacturing processes (Al-SiC MMC). Stir casting is the simplest, least expensive, and most widely used procedure among the many ways. By Stir Casting, Fin Specimens made with varied volume percentages of SiC (5, 10, and 15%) in Al and Al as a base matrix. The rectangular fin's cross-sectional area was 40 mm x 3 mm, and its length was 100 mm. Experiments were conducted across a rectangular fin with lateral circular holes of varied porosities of 0.028, 0.038, 0.050, and 0.064, as well as variable flow rates from 4-7 m/s in 1 m/s increments. The design optimization parameters and associated levels were evaluated by using Taguchi L16 experimental design method. The heat transfer of the Al-SiC nanocomposite was improved by increasing the volume percent ofSiC particles, according to the findings. For porosity 0.064 friction factor and pressure drop, a combination of 85 percent Al-15 percent SiC produced a high heat transfer coefficient and enhanced heat transfer rate as compared to standard aluminum. The optimal results were discovered for a fin composed of 85 percent Al-15 percent SiC, which compares favorably to conventional fin materials while being lighter and stronger than any of them. Investigating the fin's porosity, velocity, and composition yielded the best findings. The velocity, porosity, and composition have a greater influence on the heat transfer coefficient and Nusselt number, according to research.***

Keywords: Heat transfer coefficient, Perforations, Taguchi, Heat transfer, Nusselt number

Nomenclature

A_T: total heat transfer area (m^2)
Lc: Characteristic length of the fin (m)
H: hin height (m)
t: thickness of fin (m)
L: length of fin (m)
hav: average heat transfer coefficient (W/m^2 K)
Ka: thermal conductivity of air (W/m K)
Nu: average Nusselt number
Q: net heat transfer rate (W)
Re: Reynolds number
N_P: number of perforations
Tin: temperature of inlet air (°C)
Tout: temperature of outlet air (°C)
Tmean: mean bulk temperature (°C)
Ts: average surface temperature of fin (°C)
V: velocity over test section (m/s)
Vvoid: void volume (m^3)
Vsolid: volume of solid fin (m^3)

Greek Symbols

μ: viscosity of air (kg/ms)
ρa: density of air (kg/m^3)
Ø: porosity

1. Introduction

Scientists and Engineers are always working to enhance the qualities of their materials. This gave rise to a new type of materials known as composite materials, which are made up of two or more separate parts that differ in composition and are insoluble in each other. The matrix is a continuous phase in composite materials, whereas the reinforcement is a dispersed, non-continuous phase. Fibers, particles, or flakes can be used as reinforcing phase materials. Materials in the matrix phase are usually continuous. Each substance in a composite preserves its original qualities, but when combined, they produce greater properties that cannot be achieved alone [1]. Such materials are created to meet certain mechanical qualities that cannot be obtained from standard materials.

Aluminum-matrix composites are not made up of a single component but a family of materials whose stiffness, strength, density, thermal and electrical properties can be tailored. The Al-SiC MMC possess wide range of physical and mechanical properties such as high strength, stiffness, low density, high corrosion, wear resistance, low thermal shock, high electrical and thermal conductivity, good thermal properties and good damping capability. Among all materials, composite materials have the potential to replace widely used steel and aluminum, and many times with better performance. Al-SiC MMC's are used in various fields. The manufacturing methods available for Al-SiC MMC can be broadly classified into three types. They are powder metallurgy and diffusion bonding, liquid phase processes such as stir casting and semi-solid method [2]. Stir casting is widely regarded as a promising production technology due to its inexpensive cost, little reinforcing damage, and the fact that stir cast components are not limited in size or shape [3]. It also has advantages such as simplicity, flexibility, and suitability for large-scale production [4].

We used aluminum as the metal matrix and SiC as the reinforcement in this study. Stir Casting Process is a cost-effective method for producing Al-Si Ccomposite. Rectangular fin with lateral circular perforations ranging in size from 12-18 mm in 2 mm increments (porosity are 0.028, 0.038, 0.050, and 0.064). The rectangular fin's cross-sectional area was 40 mm x 3 mm, its length is 100 mm, as well as the flowrate was 4-7 m/s in 1m/s increments. The design optimization characteristics and their levels were examined using the Taguchi L16 experimental [5] design method. In many practical applications, determining the economic advantages of improved heat transmission is critical. As a result, the purpose of this study is to use Taguchi experimental design to minimize the number of experimental trials required to determine the heat transfer rate of perforated fins [6] and to discover new design parameters and levels.

2. Experimental Test Set Up and Design

2.1 Experimental Test Set Up

- **Stir Casting Apparatus Setup**

The major components of the Stir casting equipment [8] are shown in Fig.1. Motor, Stirrer, Crucible, Melt Base Metal (Al), Reinforcement (SiC) [7], Furnace, and Stirrer Blade.

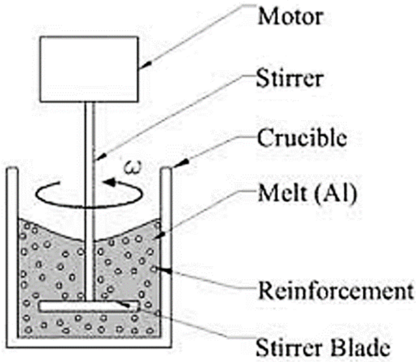

Figure 1: Stir Casting Apparatus

For the purpose of metal reinforcing Stirring duration and pace are critical; otherwise, reinforcement would settle to the bottom or on one side. The reinforcing material is injected into the matrix in order to enhance or degrade its characteristics [9]. This research is focused on composites of various compositions. Fig.2 depicts a stir casting furnace Fig. 2 (b). For improved reinforcement bonding with the matrix, the stirrer depicted in Fig.2 (g) is used to reinforce the reinforcement in the matrix.

(a) (b) (c)

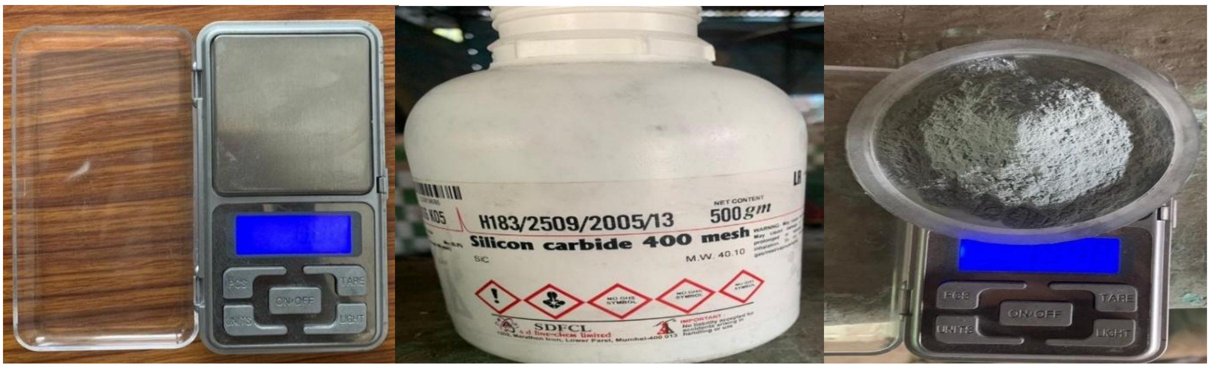

(d) (e) (f)

Paper ID: SR22612130535 DOI: 10.21275/SR22612130535

International Journal of Science and Research (IJSR)
ISSN: 2319-7064
SJIF (2022): 7.942

(g) (h) (i)

Figure 2: Stir casting procedure (a) Aluminum (b) Furnace (c) Casted Al Plates (d) Weight Machine (e) SiC Powder (f) Measured Graphite Powder (g) Stirrer (h)Stirrer with furnace (i) Al-SiC MMC Plates

The aforesaid process is employed to make components in the aluminum matrix [10] with varied SiC reinforcement proportions 5 percent, 10 percent, and 15 percent in 95 percent Al, 90 percent Al, and 85 percent Al. Table 1 lists the compositions that were created.

Table 1: The compositions

S. No	Composition (%)
1	AL
2	95%AL+5%SiC
3	90%AL+10%SiC
4	85%AL+15%SiC

- **Pin Fin Apparatus Setup**

Fig. 3 depicts the experimental setup. The Duct, Heater, Data Unit, and Plate Fin are all essential components of the arrangement.

Figure 3: Pin fin Apparatus

In the rectangular duct of the pin fin apparatus illustrated in Fig.3, a fin with a rectangular cross-section of length=100mm, width=40mm, and thickness t=3mm is fitted. The base of the fin is attached to a heater, which is used to heat the fin. Temperature sensors are installed on the fin's surface to measure the temperature. A draught fan is installed in the duct to regulate airflow with the aid of a regulator. To determine the air velocity via the duct, an anemometer has been provided. A digital wattmeter has been given to know the heater's input power.

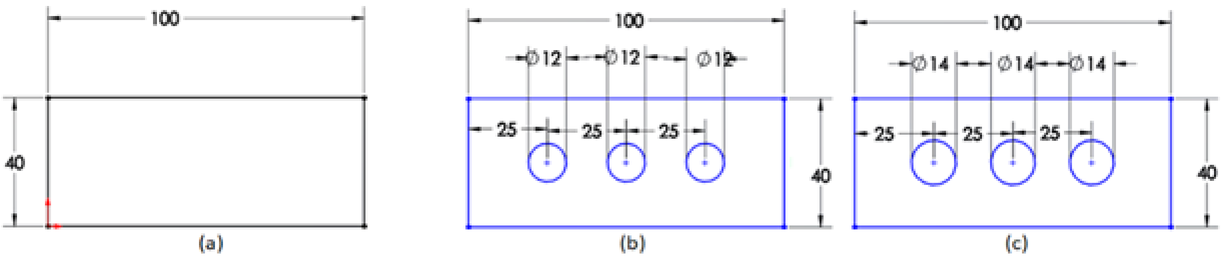

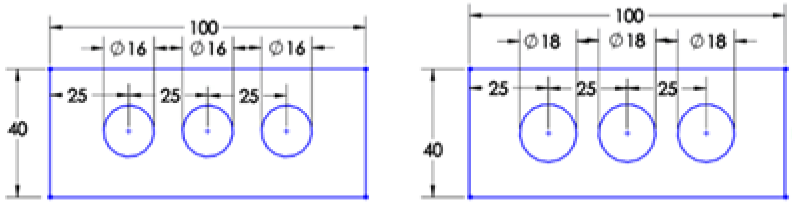

(d) (e)

Figure 4 (a): Types of fins (a) Plane fin, Perforated fins (3 perforations) (b) porosity =0.028 (c) porosity =0.038 (d) porosity =0.050 and (e) porosity =0.064.

(a) (b) (c)

Figure 4 (b): Types of fins (a) Perforated 85%Al-15%SiCfins (b) Perforated 90%Al-10%SiCfins (c) Perforated 95%Al-5%SiCfins. In above three cases perforations vary from 12mm - 18mm diameter.

Fig. 4 (a) & 4 (b) depicts the many types of fins, such as plane and perforated fins. Perforations of various porosities and compositions are

- No. of perforations: 3
- Type of fin: Without perforation & With perforation
- Composition: Al, 95%Al+5%SiC, 90%Al+10%SiC & 85%Al+15%SiC
- Size of perforation: 12, 14, 16 & 18
- Porosity: 0.028, 0.038, 0.05 & 0.064

2.2 Experimental Design

Taguchi Technique: Because of its wide variety of applications, the Taguchi approach is commonly used in industrial and engineering disciplines. The Taguchi technique is the most widely used method for enhancing design parameters [11]. The approach was initially offered as a way to improve product quality by combining statistical and technical considerations. This method is founded on two key concepts: The first is that quality losses must be clearly identified as deviations from the aims, not arbitrary specifications, and the second is that achieving high system quality levels meticulously implies quality to be built into the product. Taguchi advocates a three-stage procedure to achieve required product quality via design: system design, parameter design, and tolerance design [15].

The use of Signal-to-Noise (S/N) ratios for the same phases of the analysis is strongly recommended by Taguchi. The S/N ratio is a loss function-connected concurrent quality measurement method. The loss associated with the procedure can be avoided by optimizing the S/N ratio. From the diversity in the findings, the S/N ratio identifies the most resilient set of operational circumstances. It is handled as an experiment response parameter. The experimental data is converted to a signal-to-noise ratio (S/N). Depending on the sort of features, several S/N ratios are available. Eqs classify the S/N ratio features into three categories.

Smaller is the better characteristic: $\frac{S}{N} = -10log\left(\frac{1}{n}\sum_{i=1}^{n} Y^2\right)$

Nominal the better characteristic: $\frac{S}{N} = -10log\left(\frac{1}{n}\sum_{i=1}^{n} \frac{\bar{Y}}{S_{yi}^2}\right)$

Larger the better characteristic $\frac{S}{N} = -10log\left(\frac{1}{n}\sum_{i=1}^{n} \frac{1}{Y_i^2}\right)$

$\bar{Y}$ is the average of the observed data. S_{yi}^2 represents Y variation, The number of observations is denoted by the letter n., and Y represents the observed data. As indicated in Table 2, the number of holes on the lateral surface of the fins (porosity), velocity, and fin thickness were chosen as control factors with their values.

Table 2: Control Parameters and Their Levels

Control Parameter	Level I	Level II	Level III	Level IV
Velocity	4	5	6	7
Porosity	0.028	0.038	0.050	0.064
Composition	Al	95%Al+ 5%SiC	90%Al+ 10%SiC	85%Al+ 15%SiC

Table 3: Orthogonal array L_{16}

Expt. Trials	Velocity (V)	Porosity (Ø)	Composition (%)
1	4	0.028	Al
2	4	0.038	95%Al+5% SiC
3	4	0.050	90%Al+10% SiC
4	4	0.064	85%Al+15% SiC
5	5	0.028	95%Al+5% SiC
6	5	0.038	Al
7	5	0.050	85%Al+15% SiC
8	5	0.064	90%Al+10% SiC
9	6	0.028	90%Al+10% SiC
10	6	0.038	85%Al+15% SiC
11	6	0.050	Al
12	6	0.064	95%Al+5% SiC
13	7	0.028	85%Al+15% SiC
14	7	0.038	90%Al+10% SiC
15	7	0.050	95%Al+5% SiC
16	7	0.064	Al

Table 3 shows the Taguchi experimental design strategy that was chosen. This strategy is the most appropriate for the optimal working circumstances under investigation. An L16 orthogonal array can deliver good experimental performance with a minimum number of experimental trials, according to the Taguchi technique. For each combination of control parameters, the Nusselt number was computed using the experimental method, and the S/N ratio was determined.

2.3. Data Processing

The heat delivered to the flow by forced convection in steady-state circumstances is referred to as the net heat transfer rate Q. Eq. may be used to compute the convective heat transfer between the fin with perforations and fin without perforations arrays. $Q \;= h \;\; A_T \left[T_s - \left(\frac{T_{Out} + T_{in}}{2}\right)\right]$

The area A_T in Eq. is the entire surface area of heat transfer that comes into touch with the fluid moving through the duct

$$A_T = N_f \left[2HL + Lt - \left(\frac{\pi}{2} d^2\right) N_p + \pi dt N_p\right] \text{Perforated fin}$$

$$A_T = N_f [2Ht + 2HL + Lt] \text{Solid fin}$$

L and H are the fin's length and height, respectively, while t is its thickness and N_f is the number of fins.

The dimensionless groups are determined in the following manner. : $Nu = \frac{h \;\; L_c}{K_a}$

The Nusselt Number value (Nu) is based on the overall heat transfer area and simulates the influence of surface area differences as well as flow disorder caused by the fin shape on heat transfer. The Reynolds number (Re) is calculated using the duct's hydraulic diameter and averaged flow entrance velocity. $Re = \frac{\rho_a V D_h}{\mu}$

The volume of perforations divided by the volume of solid fins is known as porosity Porosity$\emptyset = \frac{Volume \;\; _{Void}}{Volume \;\; _{Solid}}$

The mean temperature is used in all computations to derive the values of thermophysical characteristics of air. $T_{Mean} = \frac{T_{Out} + T_{In}}{2}$

3. Result and Discussion

Table 4 shows the computed experimental values for the fin with and without perforation, as well as the outcomes.

Table 4: Experimental values for the fin with and without perforation

Type of fin	Velocity (V)	Porosity (Ø)	Composition (%)	Average Nusselt number (Nu)	Average heat transfer coefficient (h)	Heat transfer (Q)	Friction Factor	Pressure Drop
Without perforation	4	-	Al	63.2	14.93	10.37	0.0090	0.0359
With perforation	4	0.028	Al	60.6	15.59	11.06	0.0094	0.0375
With perforation	4	0.038	95%Al+5% SiC	59.7	15.88	11.37	0.0095	0.0381
With perforation	4	0.050	90%Al+10% SiC	58.5	16.23	11.72	0.0097	0.0389
With perforation	4	0.064	85%Al+15% SiC	57.2	16.65	12.13	0.0100	0.0399
With perforation	5	0.028	95%Al+5% SiC	67.3	17.30	12.37	0.0084	0.0335
With perforation	5	0.038	Al	66.2	17.62	12.67	0.0085	0.0341
With perforation	5	0.050	85%Al+15% SiC	65.0	18.01	13.09	0.0087	0.0348
With perforation	5	0.064	90%Al+10% SiC	63.5	18.48	13.49	0.0089	0.0357
With perforation	6	0.028	90%Al+10% SiC	73.2	18.84	13.51	0.0077	0.0306
With perforation	6	0.038	85%Al+15% SiC	72.1	19.18	13.87	0.0078	0.0311
With perforation	6	0.050	Al	70.7	19.60	14.22	0.0079	0.0318
With perforation	6	0.064	95%Al+5% SiC	69.1	20.12	14.77	0.0081	0.0326
With perforation	7	0.028	85%Al+15% SiC	78.7	20.24	14.33	0.0071	0.0283
With perforation	7	0.038	90%Al+10% SiC	77.4	20.61	14.93	0.0072	0.0288
With perforation	7	0.050	95%Al+5% SiC	76.0	21.06	15.34	0.0074	0.0294
With perforation	7	0.064	Al	74.3	21.61	14.82	0.0075	0.0301

Table 5 illustrates the percentage increase in heat transfer coefficient h and heat transfer rate of perforated fins over plane fins.

Table 5: Percentage increase in heat transfer coefficient and heat transfer rate of perforated fin over the plane fin.

Type of fin	Velocity (V)	Porosity (∅)	Composition (%)	Percentage increase 'h' over plan fin	Percentage increase 'Q' over plan fin
Without perforation	4	-	Al	-	-
With perforation	4	0.028	Al	4.44	6.65
With perforation	4	0.038	95%Al+5% SiC	6.36	9.71
With perforation	4	0.050	90%Al+10% SiC	8.70	13.08
With perforation	4	0.064	85%Al+15% SiC	11.54	16.96
With perforation	5	0.028	95%Al+5% SiC	15.89	19.31
With perforation	5	0.038	Al	18.01	22.19
With perforation	5	0.050	85%Al+15% SiC	20.61	26.23
With perforation	5	0.064	90%Al+10% SiC	23.76	30.12
With perforation	6	0.028	90%Al+10% SiC	26.16	30.29
With perforation	6	0.038	85%Al+15% SiC	28.48	33.76
With perforation	6	0.050	Al	31.30	37.16
With perforation	6	0.064	95%Al+5% SiC	34.73	42.42
With perforation	7	0.028	85%Al+15% SiC	35.56	38.22
With perforation	7	0.038	90%Al+10% SiC	38.05	43.96
With perforation	7	0.050	95%Al+5% SiC	41.08	47.99
With perforation	7	0.064	Al	44.77	42.92

We may deduce from Table 5 that perforating a plane fin while altering velocity, perforation size, and composition enhances the percentage increase in convective heat transfer coefficient and heat transfer rate. We used the Taguchi technique to discover the best ideal design. The S/N ratio for the L16 orthogonal array is shown in Table 6. All of the experiential values in the Taguchi technique are derived with the assumption that the larger the better.

Taguchi Analysis

Heat transfer coefficient h, heat transfer rate vs Velocity (V), porosity (), and material composition as a percentage increase.

Table 6: S/N ratio for L16 orthogonal array (heat transfer coefficient h, heat transfer rate versus Velocity (V), Porosity (∅), Material composition)

Exp. Trials	Velocity (V)	Porosity (∅)	Composition (%)	Percentage increase over plan fin %h	SNRA1 for '%h'	Percentage increase over plan fin %Q	SNRA2 For '%Q'	SNRA3 For '%h & %Q'
1	4	0.028	Al	4.44	12.9526	6.65	16.4501	14.3584
2	4	0.038	95%Al+5% SiC	6.36	16.0656	9.71	19.7433	17.5263
3	4	0.050	90%Al+10% SiC	8.70	18.7877	13.08	22.3321	20.2079
4	4	0.064	85%Al+15% SiC	11.54	21.2415	16.96	24.5910	22.6010
5	5	0.028	95%Al+5% SiC	15.89	24.0212	19.31	25.7171	24.7869
6	5	0.038	Al	18.01	25.1115	22.19	26.9240	25.9239
7	5	0.050	85%Al+15% SiC	20.61	26.2810	26.23	28.3758	27.2033
8	5	0.064	90%Al+10% SiC	23.76	27.5166	30.12	29.5763	28.4255
9	6	0.028	90%Al+10% SiC	26.16	28.3541	30.29	29.6252	28.9433
10	6	0.038	85%Al+15% SiC	28.48	29.0900	33.76	30.5687	29.7667
11	6	0.050	Al	31.30	29.9119	37.16	31.4012	30.5930
12	6	0.064	95%Al+5% SiC	34.73	30.8150	42.42	32.5515	31.5970
13	7	0.028	85%Al+15% SiC	35.56	31.0193	38.22	31.6458	31.3213
14	7	0.038	90%Al+10% SiC	38.05	31.6062	43.96	32.8618	32.1887
15	7	0.050	95%Al+5% SiC	41.08	32.2732	47.99	33.6225	32.8957
16	7	0.064	Al	44.77	33.0194	42.92	32.6530	32.8323

- S/N Response Table 7: Percentage increase in convective heat transfer coefficient over plan fin vs Velocity (v), Porosity (∅), and Composition (%)
  Taguchi Analysis: Percentage increase over plan fin h versus Velocity (v), Porosity (∅), Composition (%)

Table 7: Response Table for Signal to Noise Ratios: Larger is better

Level	Velocity (v)	Porosity (∅)	Composition (%)
1	17.26	24.09	26.91
2	25.73	25.47	26.57
3	29.54	26.81	25.79
4	31.98	28.15	25.25
Delta	14.72	4.06	1.66
Rank	1	2	3

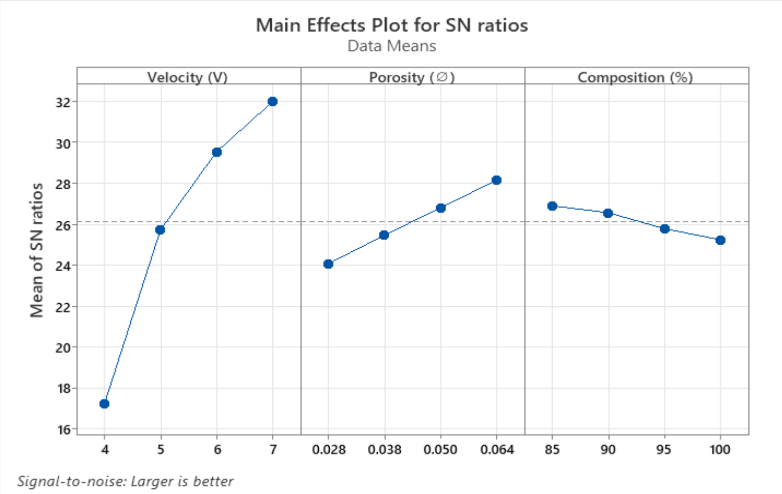

Figure 5: Signal to Noise Ratios (% increase over plan fin h versus Velocity (v), Porosity (∅), Composition (%))

According to Fig. 5, the optimum level design made this possible for a percentage increase in convective heat transfer coefficient over plan fin is V4, ∅4 & for Composition4, with the values of each parameter being V4 i.e., Velocity diameter is 7 m/s, ∅4 i.e., Porosity of fin is 0.064mm i.e., 18mm perforation diameter, and Composition4 i.e., Composition of the fin is 85%Al+15%SiC.

- S/N Response Table 8: percentage increase of heat transfer Q over plan fin vs Velocity (v), Porosity (∅), and Composition (%)

Taguchi Analysis: percentage increase heat transfer Q over plan fin versus Velocity (v), Porosity (∅), Composition (%)

Table 8: Response Table for Signal to Noise Ratios: Larger is better

Level	Velocity (v)	Porosity (∅)	Composition (%)
1	20.78	25.86	28.80
2	27.65	27.52	28.60
3	31.04	28.93	27.91
4	32.70	29.84	26.86
Delta	11.92	3.98	1.94
Rank	1	2	3

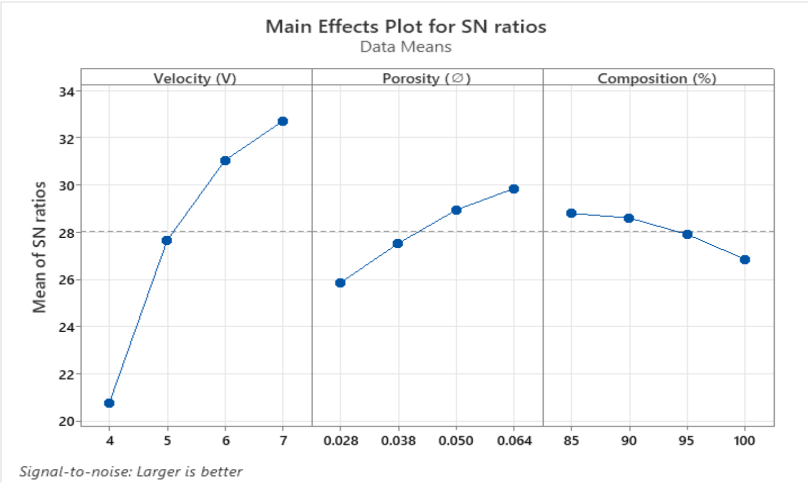

Figure 6: Signal to Noise Ratios (% increase of heat transfer Q over plan fin versus Velocity (v), Porosity (∅) & Composition (%))

According to Fig. 6, the optimum level design made this possible for a percentage increase in heat transfer Q over plan fin is V4, ∅4 & for Composition4, with the values of each parameter being V4 i.e., Velocity diameter is 7 m/s, ∅4 i.e., Porosity of fin is 0.064mm i.e., 18mm perforation diameter, and Composition4 i.e., Composition of the fin is 85%Al+15%SiC

- S/N Response Table 9: Percentage increase over plan fin h, % increase over plan fin Q vs Velocity (v), Porosity (∅), and Composition (%)

Taguchi Analysis: Percentage increase over plan fin h, % increase over plan fin Q versus Velocity (v), Porosity (∅), Composition (%).

Table 9: Response Table for Signal to Noise Ratios: Larger is better

Level	Velocity (v)	Porosity (∅)	Composition (%)
1	18.67	24.85	27.72
2	26.58	26.35	27.44
3	30.23	27.72	26.70
4	32.31	28.86	25.93
Delta	13.64	4.01	1.80
Rank	1	2	3

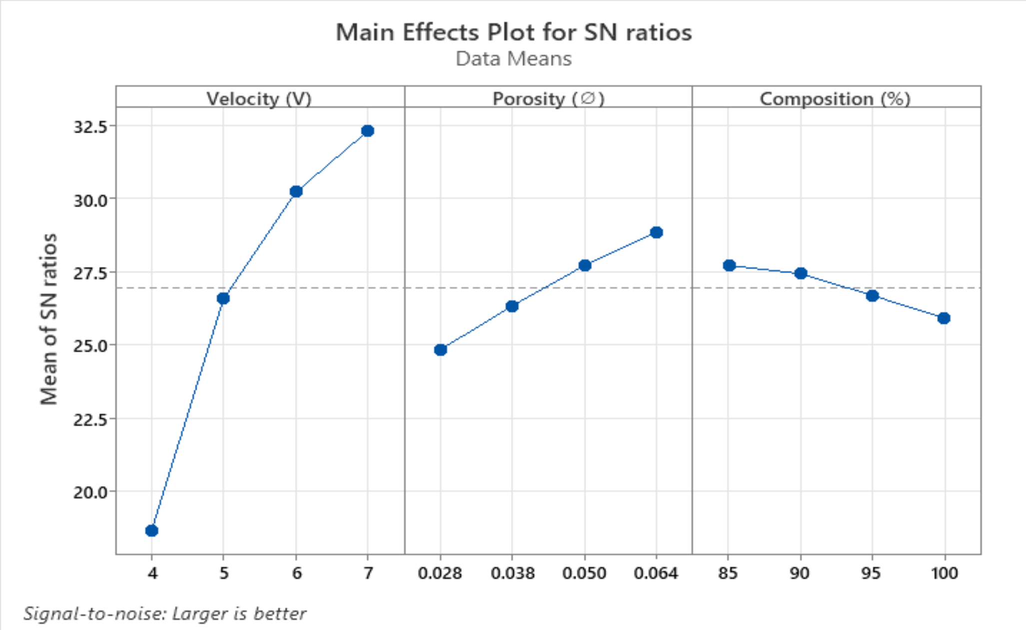

Figure 7: Signal to Noise Ratios (% increase over plan fin h, % increase over plan fin Q versus Velocity (v), Porosity (Ø), Composition (%))

According to Fig. 7, the optimum level design made this possible for a percentage increase inheat transfer coefficient h, heat transfer rate Q over plan fin is V4, Ø4 & for Composition4, with the values of each parameter being V4 i.e., Velocity diameter is 7 m/s, Ø4 i.e., Porosity of fin is 0.064mm i.e., 18mm perforation diameter, and Composition4 i.e., Composition of the fin is 85%Al+15%SiC

The S/N ratio for the L16 orthogonal array is shown in Table 10. All of the experiential values in the Taguchi approach are computed with the assumption that the larger the better. The friction factor [14] and pressure drop experienced values will be set to the maximum in this study.

Table 10: S/N ratio for L16 orthogonal array for friction factor and pressure drop

Type of fin	Velocity (V)	Porosity (Ø)	Composition (%)	Friction Factor	SNRA4 for Friction Factor	Pressure Drop	SNRA5 for Pressure Drop
With perforation	4	0.028	Al	0.0094	-40.5626	0.0375	-28.5214
With perforation	4	0.038	95%Al+5% SiC	0.0095	-40.4149	0.0381	-28.3737
With perforation	4	0.050	90%Al+10% SiC	0.0097	-40.2379	0.0389	-28.1967
With perforation	4	0.064	85%Al+15% SiC	0.0100	-40.0282	0.0399	-27.9870
With perforation	5	0.028	95%Al+5% SiC	0.0084	-41.5317	0.0335	-29.4905
With perforation	5	0.038	Al	0.0085	-41.3840	0.0341	-29.3428
With perforation	5	0.050	85%Al+15% SiC	0.0087	-41.2070	0.0348	-29.1658
With perforation	5	0.064	90%Al+10% SiC	0.0089	-40.9973	0.0357	-28.9561
With perforation	6	0.028	90%Al+10% SiC	0.0077	-42.3235	0.0306	-30.2823
With perforation	6	0.038	85%Al+15% SiC	0.0078	-42.1758	0.0311	-30.1346
With perforation	6	0.050	Al	0.0079	-41.9988	0.0318	-29.9576
With perforation	6	0.064	95%Al+5% SiC	0.0081	-41.7891	0.0326	-29.7479
With perforation	7	0.028	85%Al+15% SiC	0.0071	-42.9930	0.0283	-30.9518
With perforation	7	0.038	90%Al+10% SiC	0.0072	-42.8452	0.0288	-30.8040
With perforation	7	0.050	95%Al+5% SiC	0.0074	-42.6683	0.0294	-30.6271
With perforation	7	0.064	Al	0.0075	-42.4585	0.0301	-30.4173

- S/N Response Table 11: Friction Factor vs Velocity (v), Porosity (Ø), and Composition (%)

Taguchi Analysis: Friction Factor versus Velocity (v), Porosity (Ø), Composition (%)

Table 11: Response Table for Signal to Noise Ratios: Larger is better

Level	Velocity (v)	Porosity (Ø)	Composition (%)
1	-40.31	-41.85	-41.60
2	-41.28	-41.70	-41.60
3	-42.07	-41.53	-41.60
4	-42.74	-41.32	-41.60
Delta	2.43	0.53	0.00
Rank	1	2	3

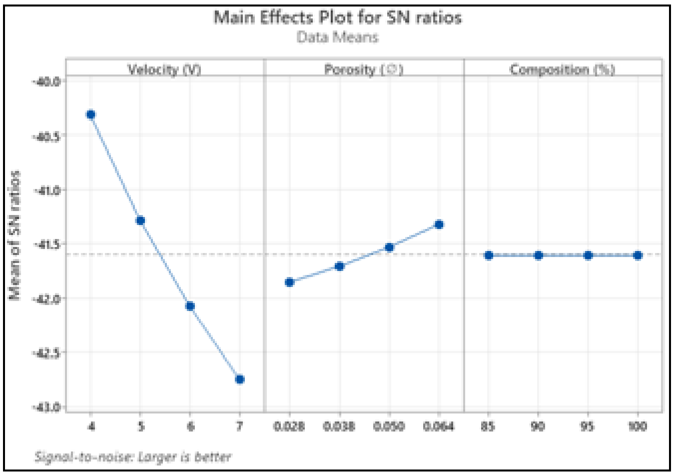

Figure 8: Signal to Noise Ratios (Friction Factor versus Velocity (v), Porosity (∅), Composition (%))

Figure 8 is an excellent demonstration that when velocity rises, the friction factor decreases. At low speeds, the friction factor is significant, while at high speeds, it is low. The friction factor increases as the porosity increases, reaching a maximum at 0.064 and a minimum at 0.028, while the proportion of composition has no effect on the friction factor.

- S/N Response Table 12: Pressure drop vs Velocity (v), Porosity (∅), and Composition (%)

Taguchi Analysis: Pressure drop versus Velocity (v), Porosity (∅), Composition (%)

Table 12: Response Table for Signal to Noise Ratios: Larger is better

Level	Velocity (v)	Porosity (∅)	Composition (%)
1	-28.27	-29.81	-29.56
2	-29.24	-29.66	-29.56
3	-30.03	-29.49	-29.56
4	-30.70	-29.28	-29.56
Delta	2.43	0.53	0.00
Rank	1	2	3

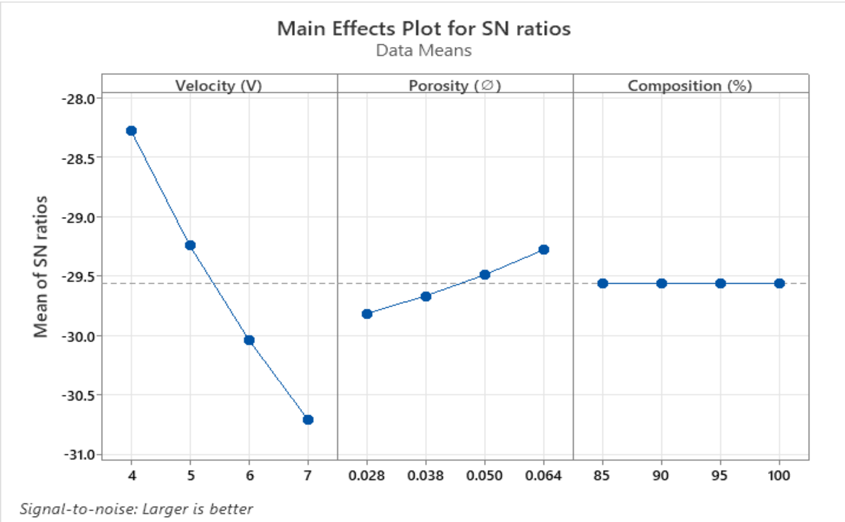

Figure 9: Signal to Noise Ratios (Pressure drop versus Velocity (v), Porosity (∅), Composition (%))

Figure 9 illustrates when velocity rises, the pressure drop reduces. The pressure drop is high at low speeds and minimal at high speeds. The pressure drop increases as the porosity increases, reaching a maximum at 0.064 and a minimum at 0.028, while the proportion of composition has no effect on the pressure drop.

4. Conclusion

According to the findings, perforating a plane fin and altering velocity, porosity, and composition enhances the heat transfer coefficient, heat transfer rate, friction factor, and pressure drop. With the Taguchi Method, we can achieve the optimal answer with a smaller number of trials. According to the research done on Taguchi L16 orthogonal arrays, the velocity of the fin is the most important factor determining the heat transfer coefficient, followed by porosity and then composition fins. The highest heat transfer rate limit is practicable for 3 mm fin thickness and 7 m/s airflow velocities, 0.064 porosity in fin, and for the composition 85%Al+15%SiC. As a result, it's reasonable to conclude that by enhancing these parameters, heat transfer can be efficiently increased. The pressure drop diminishes as the velocity increases and the friction factor lowers. Because of the friction factor, the pressure loss is considerable at low speeds and low at high speeds. The friction factor, pressure drop increases as the porosity increases, with a maximum at 0.064 and a minimum at 0.028, while the proportion of composition has no effect on the friction factor or pressure drop. As a consequence, we believe that using the L16 Orthogonal Array Method will yield an incomparable result with fewer trials and is also cost-effective.

Acknowledgement

The author (Mr. A. Kalyan Charan, Assistant Professor, Dept. of Mechanical Engineering, and MECS) wishes to express his gratitude to the management and principal of Matrusri Engineering College (MECS) for their encouragement and permission to conduct this research.

References

[1] M K Surappa, "Aluminium Matrix Composites: Challenges and Opportunities", Sadhana Vol. 28, Parts 1 & 2, February/April 2003, pp 319-334.

[2] S. Naher, D Brabazon and L Looney, "Development and Assessment of a New Quick Quench Stir Caster Design for the Production of MetalMatrix Composites", Journal of Material Processing Technology, Vol. 166, 2004, pp 430-439.

[3] J. Hashim, L Looney and M S J Hashmi, "Metal Matrix Composites: Production by the Stir Casting Method", Journal of MaterialProcessing and Technology, Vol. 92, 1999, pp 1-7.

[4] Y. H. Seo and C. G. Kang, "Effects of Hot Extrusion Through a Curved Die on the Mechanical Properties of Al-SiC Composites Fabricatedby Melt-Stirring", Composites Science and Technology, Vol.59, 1999, pp 643-654.

[5] Ashok Kumar Sahoo, Swastik Pradhan, "Modeling and optimization of Al/SiCp MMC machining using Taguchi approach" Elsevier Measurement, Volume 46, Issue 9, 2013, Pages 3064-3072, ISSN 0263-2241

[6] Ahmadi Nadooshan, A., Kalbasi, R. & Afrand, M. "Perforated fins effect on the heat transfer rate from a circular tube by using wind tunnel: An experimental view". Heat Mass Transfer 54, 3047-3057 (2018).

[7] M. Patel, B. Pardhi, M. Pal, and M. K. Singh, "SiC Particulate Reinforced Aluminium Metal Matrix Composite", Adv. J. Grad. Res., vol. 5, no. 1, pp. 8-15, Sep. 2018.

[8] V. Mohanavel, K. Rajan, P. V. Senthil, S. Arul, "Mechanicalbehaviour of hybrid composite (AA6351+Al2O3+Gr) fabricated by stir casting method", Materials Today: Proceedings, Volume 4, Issue 2, Part A, 2017, Pages 3093-3101, ISSN 2214-7853.

[9] Dipen Kumar Rajak, Durgesh D. Pagar, Ravinder Kumar, Catalin I. Pruncu, " Recent progress of reinforcement materials: a comprehensive overview of composite materials", Journal of Materials Research and Technology, Volume 8, Issue 6, 2019, Pages 6354-6374, ISSN 2238-7854.

[10] Arunkumar K N, Dr. G B Krishnappa, "Mechanical Properties of Aluminum Metal Matrix Composites - A Review", International Journal of Engineering Research & Technology (IJERT) Volume 11, Issue 03 (March 2022).

[11] Patyal VS, Modgil S, Maddulety K. "Application of Taguchi Method of Experimental Design for Chemical Process Optimisation: A Case Study". Asia-Pacific Journal of Management Research and Innovation. 2013; 9 (3): 231-238.